Roles for *Nkx3.1* in prostate development and cancer

Rajula Bhatia-Gaur,[1,2] Annemarie A. Donjacour,[4] Peter J. Sciavolino,[1,2,7] Minjung Kim,[1,2] Nishita Desai,[1,3] Peter Young,[4] Christine R. Norton,[5] Thomas Gridley,[5] Robert D. Cardiff,[6] Gerald R. Cunha,[4] Cory Abate-Shen,[1,2,8] and Michael M. Shen[1,3,8]

[1]Center for Advanced Biotechnology and Medicine, [2]Department of Neuroscience and Cell Biology and [3]Department of Pediatrics, University of Medicine and Dentistry of New Jersey (UMDNJ)–Robert Wood Johnson Medical School, Piscataway, New Jersey 08854 USA; [4]Department of Anatomy, University of California, San Francisco, California 94143 USA; [5]The Jackson Laboratory, Bar Harbor, Maine 04609 USA; [6]Department of Pathology, School of Medicine, University of California, Davis, California 95616 USA

In aging men, the prostate gland becomes hyperproliferative and displays a propensity toward carcinoma. Although this hyperproliferative process has been proposed to represent an inappropriate reactivation of an embryonic differentiation program, the regulatory genes responsible for normal prostate development and function are largely undefined. Here we show that the murine *Nkx3.1* homeobox gene is the earliest known marker of prostate epithelium during embryogenesis and is subsequently expressed at all stages of prostate differentiation in vivo as well as in tissue recombinants. A null mutation for *Nkx3.1* obtained by targeted gene disruption results in defects in prostate ductal morphogenesis and secretory protein production. Notably, *Nkx3.1* mutant mice display prostatic epithelial hyperplasia and dysplasia that increases in severity with age. This epithelial hyperplasia and dysplasia also occurs in heterozygous mice, indicating haploinsufficiency for this phenotype. Because human *NKX3.1* is known to map to a prostate cancer hot spot, we propose that *NKX3.1* is a prostate-specific tumor suppressor gene and that loss of a single allele may predispose to prostate carcinogenesis. The *Nkx3.1* mutant mice provide a unique animal model for examining the relationship between normal prostate differentiation and early stages of prostate carcinogenesis.

[*Key Words:* prostate; bulbourethral gland; organogenesis; hyperplasia/dysplasia; haploinsufficiency; tumor suppressor gene]

Received December 30, 1998; revised version accepted March 2, 1999.

The prostate gland is of paramount importance for human disease due to the increasing incidence of benign prostatic hyperplasia and prostate carcinoma in aging men. Prostate carcinoma now represents the second leading cause of cancer death in American men (Coffey 1992; Landis et al. 1998). Nonetheless, little is known about the molecular factors that contribute to the onset or progression of prostate cancer. A primary impediment for identifying relevant molecular factors has been the paucity of information regarding the mechanisms of normal prostate growth and differentiation. Few regulatory genes are known to be expressed specifically during prostate development or to be required for prostate function.

The prostate is a ductal gland situated at the base of the bladder that contributes secretory proteins to the seminal fluid. At maturity, the prostate is comprised of tall columnar epithelium surrounded by smooth muscle stroma (Cunha et al. 1987; Cunha 1994). Signaling interactions between epithelium and mesenchyme are required for normal prostate growth and differentiation while deranged interactions may contribute to the inappropriate reactivation of cellular proliferation that occurs during aging (McNeal 1978; Hayward et al. 1996). During embryogenesis, inductive signals from the urogenital sinus mesenchyme induce the adjacent epithelium to form prostatic buds (Cunha et al. 1987; Cunha 1994). Postnatally, reciprocal interactions between epithelium and stroma (mesenchyme) are also required for ductal morphogenesis and prostate maturation (Donjacour and Cunha 1988). At all stages of prostate development as well as maturity, these tissue interactions require functional androgen receptors, initially in the mesenchyme and subsequently in the epithelium (Cunha et al. 1987; Cunha 1994). Although it is known that reciprocal signaling interactions are responsible for prostate formation and function, the relevant molecular factors are largely undefined.

Among the few regulatory genes known to be expressed in the prostate, the *NKX3.1* homeobox gene is of

[7]Present address: SciavoTECH Research and Consultancy Services, Inc., Naples, Florida 34119 USA.
[8]Corresponding authors.
E-MAIL abate@mbcl.rutgers.edu, mshen@cabm.rutgers.edu; FAX (732) 235-4850.

particular interest because it maps to the minimal region of human chromosome 8p21 (He et al. 1997; Voeller et al. 1997) that undergoes loss of heterozygosity in 60%–80% of prostate tumors (Bergerheim et al. 1991; Bova et al. 1993; Trapman et al. 1994; Cher et al. 1996; Vocke et al. 1996). In this study we investigate the expression and function of murine *Nkx3.1* (Bieberich et al. 1996; Sciavolino et al. 1997) in the developing and mature prostate. We show that *Nkx3.1* expression during embryogenesis appears to demarcate prospective prostate epithelium prior to prostate formation and continues to mark prostate epithelium during neonatal development, as well as in tissue recombinants. Furthermore, *Nkx3.1* is required for prostate function, as null mutants generated by gene targeting display defects in ductal morphogenesis and secretory protein production. Finally, *Nkx3.1* regulates prostate epithelial proliferation, as its loss results in epithelial hyperplasia and dysplasia that increases in severity with age, modeling a preneoplastic condition. Taken together, our results link the regulatory actions of *Nkx3.1* in normal prostate development and function with its potential role in prostate carcinogenesis.

Results

Restricted expression of Nkx3.1 *in adult prostate and bulbourethral glands*

In rodents, the prostate gland consists of three lobes, the anterior prostate (AP; also known as the coagulating gland), the dorsolateral prostate (DLP), and the ventral prostate (VP) (Fig. 1A). These lobes are arranged circumferentially around the urethra and display characteristic patterns of ductal branching and protein secretion (Cunha et al. 1987). In contrast, the adult human prostate lacks discernible lobular organization and, instead, completely envelops the urethra at the base of the bladder (Cunha et al. 1987). The prostatic lobes and bulbourethral gland (BUG; also known as Cowper's gland in humans) arise from the endodermally derived urogenital sinus epithelium, whereas other ductal tissues of the male urogenital system arise from the mesodermally derived Wolffian ducts (Fig. 1A,B; Cunha et al. 1987).

We examined the distribution of *Nkx3.1* transcripts in the adult mouse, with particular emphasis on male urogenital tissues. We found by ribonuclease protection analysis that *Nkx3.1* expression was highly restricted to the three prostatic lobes and the BUG (Fig. 1C). In contrast, *Nkx3.1* transcripts were not detectable in the seminal vesicle, ampullary gland, ductus deferens, or epididymus, which are derivatives of the Wolffian duct, or in the bladder and urethra, which are nonductal derivatives of the primitive urogenital sinus. Quantitation of *Nkx3.1* transcripts demonstrated highest levels in the BUG (normalized to 100%), followed in order by the AP (47%), DLP (26%), and the VP (9%). No expression was detected in other tissues examined, consistent with previous studies (Bieberich et al. 1996; Sciavolino et al. 1997). Thus, these data demonstrate that adult expression of *Nkx3.1* is restricted to ductal derivatives of the urogenital sinus.

Nkx3.1 *expression defines early stages of prostate development*

Given the highly restricted expression of *Nkx3.1* in the AP and BUG, we investigated its expression during late stages of embryogenesis, when these tissues arise from

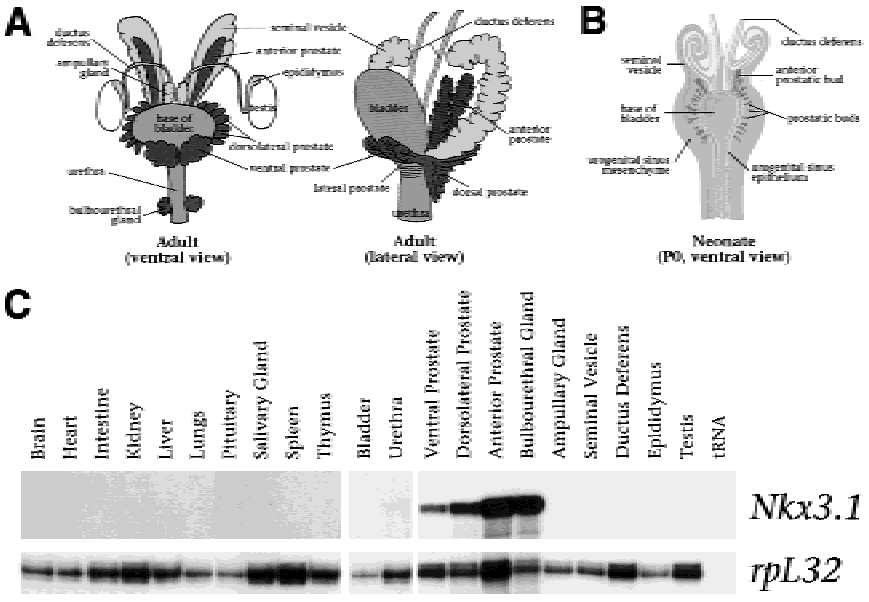

Figure 1. Prostate-specific expression of *Nkx3.1* in adult male mice. (*A*) Diagram of the male urogenital system in adult mice, showing the embryological relationships of the tissues (adapted from Cunha et al. 1987; Podlasek et al. 1997). The anterior, dorsolateral, and ventral prostatic lobes, as well as the BUGs (dark gray) are ductal derivatives of the urogenital sinus; the bladder and urethra (medium gray) are its nonductal derivatives. The seminal vesicles, ductus deferens, epididymides, and ampullary glands (light gray) are derived from the Wolffian duct, and the testes (white) from the genital ridge. In the ventral view, only the base of the bladder is shown for clarity. (*B*) Diagram of the male urogenital system in a newborn mouse [postnatal day 0 (P0; adapted from Cunha et al. 1987)]. By 17.5 dpc, the prostatic buds (dark gray) arise as outbuddings of the urogenital sinus epithelium (white) into the surrounding mesenchyme (medium gray). Also shown are the Wolffianduct-derived seminal vesicles and ductus deferens (light gray). (*C*) Ribonuclease protection analysis using total RNA (20 μg) from the indicated tissues of adult (8-week) male mice, using a *Nkx3.1* antisense riboprobe. The *rpL32* riboprobe serves as an internal control for RNA loading.

the urogenital sinus. We have examined the pattern of *Nkx3.1* expression by section in situ hybridization in male mouse embryos from 14.5 through 17.5 days postcoitum (dpc), prior to and during formation of the prostate gland and the BUG (Fig. 2A–M). Our results demonstrate that *Nkx3.1* is the earliest known molecular marker of the prostate epithelium and define initial steps in prostate formation.

During mid-gestation, the primitive urogenital sinus originates from the terminal hindgut through the division of the cloaca by the urorectal septum. The terminal regions of the primitive urogenital sinus form the urinary bladder and the penile urethra. The prostate gland and the BUG are formed from the intermediate region, which we refer to as the urogenital sinus. The prostatic lobes arise from the rostral urogenital sinus at ~17.5 dpc, whereas the BUG arise from its caudal end at ~14.5 dpc.

In the rostral urogenital sinus, *Nkx3.1* expression is first detected at 15.5 dpc, in a characteristic 'parentheses' pattern that encompasses the lateral aspects of the urogenital sinus epithelium and is excluded from its dorsal and ventral sides (Fig. 2B,C,F,G). Although the urogeni-

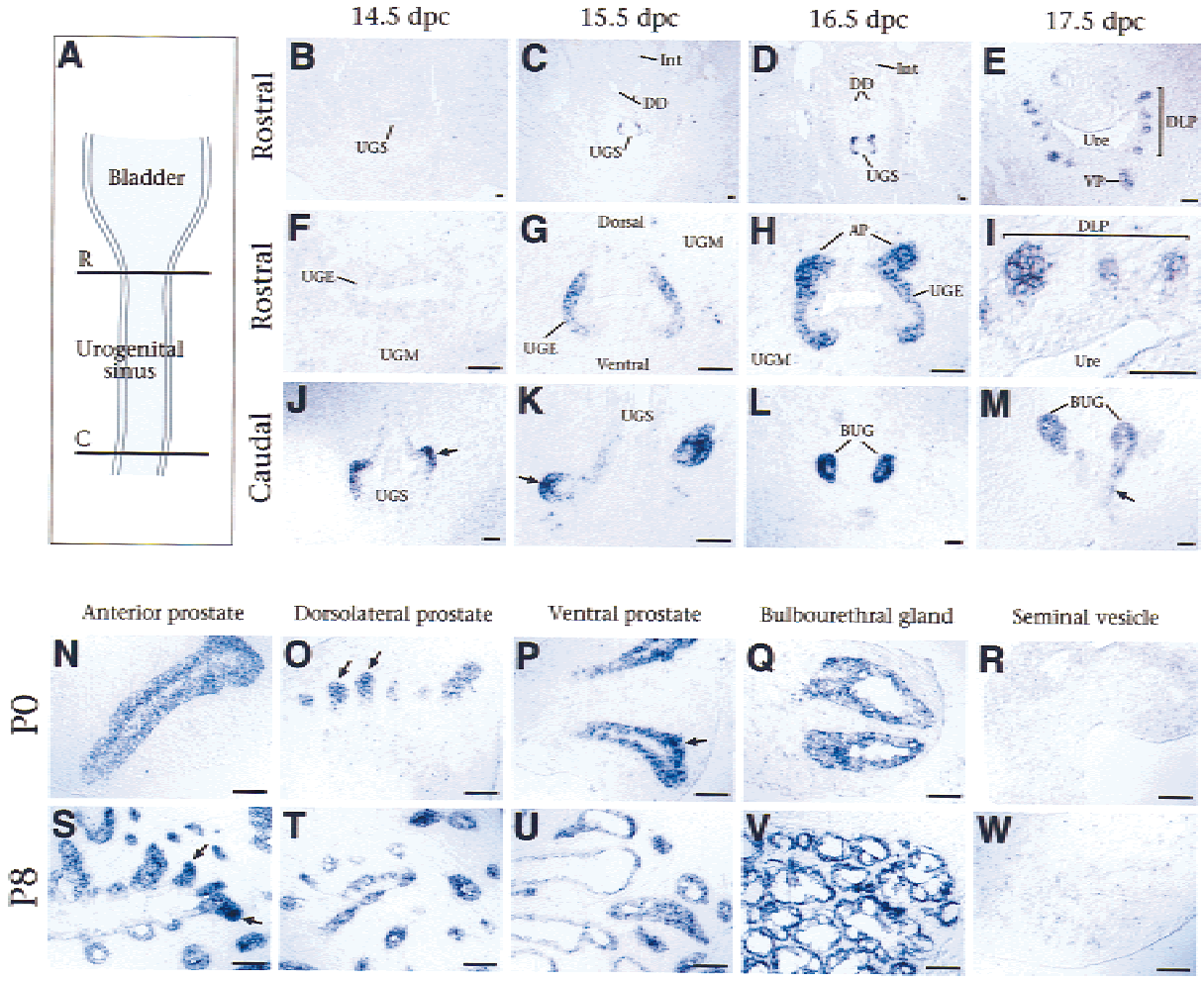

Figure 2. Expression of *Nkx3.1* in embryonic and neonatal prostate. (*A*) Diagram showing transverse planes of section through the urogenital sinus, shown in panels *B–M*. The rostral region (R) corresponds to the location of the prospective prostatic buds; the caudal region (C) corresponds to the prospective bulbourethral glands. (*B–I*) In situ hybridization analysis of *Nkx3.1* expression in transverse sections through the rostral male urogenital sinus, shown at low (*B–E*) and high (*F–I*) power. (*B*,*F*) No expression is detected at 14.5 dpc. (*C*,*G*) At 15.5 dpc, *Nkx3.1* expression is restricted to the lateral urogenital sinus epithelium (UGE) and is excluded from the dorsal and ventral sides (forming the parentheses pattern). (*D*,*H*) *Nkx3.1* expression continues in the lateral UGE, with elevated expression in the emerging anterior prostatic buds. (*E*,*I*) At 17.5 dpc, expression is restricted to the newly formed dorsolateral and ventral prostatic buds and is not found in the prospective urethral epithelium. (*J–M*) *Nkx3.1* expression in transverse sections through the caudal male urogenital sinus. (*J*) Expression at 14.5 dpc is found in bilateral outpouchings (arrow) from the UGE. (*K–M*) At 15.5–17.5 dpc, expression is found in the nascent BUGs and the ducts (arrow in *M*) that join them to the prospective urethra. (*N–W*) *Nkx3.1* expression in isolated tissues from male mice at P0 and P8; staining is more intense at the ends of the outgrowing prostatic ducts (arrows in *O*, *P*, and *S*). (AP) Anterior prostate; (BUG) bulbourethral gland; (C) caudal; (DD) ductus deferens; (DLP) dorsolateral prostate; (Int) large intestine; (R) rostral; (UGE) urogenital sinus epithelium; (UGM) urogenital sinus mesenchyme; (UGS) urogenital sinus; (Ure) urethra; (VP) ventral prostate. Scale bar, 50 µm.

tal sinus epithelium is multilayered at this stage, *Nkx3.1* is only expressed in the basal layer and not in the suprabasal layers (Fig. 2G). At 16.5 dpc, this parentheses pattern of expression becomes more intense at its dorsal boundaries, where the buds of the anterior prostate emerge (Fig. 2D,H). At 17.5 dpc, *Nkx3.1* expression becomes restricted to the epithelium of the outgrowing ventral, dorsolateral, and anterior prostatic buds and is excluded from the prospective urethral epithelium (Fig. 2E,I). Thus, *Nkx3.1* expression appears to demarcate regions where prostatic buds will arise from the urogenital sinus epithelium.

At the caudal end of the urogenital sinus, *Nkx3.1* is expressed at high levels in the epithelial buds of the BUGs (Fig. 2J–M). At 14.5 and 15.5 dpc, this expression was detected in bilateral outpouchings of the urogenital sinus epithelium into the surrounding mesenchyme (Fig. 2J,K). At 16.5 and 17.5 dpc, *Nkx3.1* continues to be expressed at high levels in the nascent BUGs, as well as in the epithelial ducts that join the glands to the prospective urethra (Fig. 2L,M).

Nkx3.1 expression is highly restricted within the embryonic male urogenital system to the rostral and caudal ends of the urogenital sinus epithelium; transcripts were not detected at any stage in the bladder or in Wolffian duct derivatives. Furthermore, this expression pattern is male-specific, as *Nkx3.1* transcripts were not detected in female urogenital sinus at any stage (data not shown). However, *Nkx3.1* expression is found in several nonsexually dimorphic tissues at earlier developmental stages (Sciavolino et al. 1997; Kos et al. 1998; Treier et al. 1998).

In rodents, the prostatic epithelial buds undergo extensive ductal outgrowth and branching during the first 3 weeks of postnatal development. *Nkx3.1* expression persists at high levels in the epithelium of all three prostatic lobes at postnatal day (P) 0, 8, and 18 (Fig. 2N–P, S–U; data not shown). Notably, expression appears highest toward the distal ends of the outgrowing ducts, corresponding to regions of active morphogenesis (arrows in Figure 2O,P,S). During this postnatal period, the BUGs also undergo extensive epithelial ductal branching within a capsular stromal layer (Cooke et al. 1987a,b). *Nkx3.1* expression continues in the epithelium of the BUGs, although it appears uniform in level throughout the ducts (Fig. 2Q,V). As is the case for embryonic development, *Nkx3.1* expression is not found in other tissues of the male urogenital system (Fig. 2R,W; data not shown). Thus, *Nkx3.1* is a specific marker for ductal outgrowth and morphogenesis during postnatal growth of the prostate.

Nkx3.1 *marks prostate epithelium in tissue recombinants*

To further examine the relationship of *Nkx3.1* expression to prostate formation, we utilized a tissue recombination system (Fig. 3A). The epithelial–mesenchymal interactions required for prostate formation can be effectively recapitulated in tissue recombinants, such that

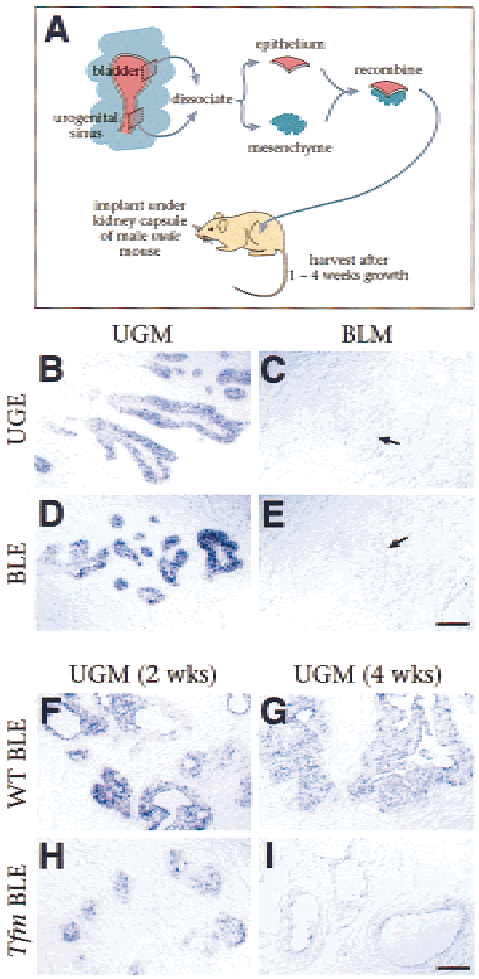

Figure 3. *Nkx3.1* marks prostate differentiation in tissue recombinants. (*A*) Design of the tissue recombination assay. Recombinants of urogenital sinus mesenchyme (UGM) with either urogenital sinus epithelium (UGE) or bladder epithelium (BLE) form prostate; recombinants of bladder mesenchyme (BLM) with either epithelium form bladder. (*B–E*) In situ hybridization analysis of *Nkx3.1* expression in tissue recombinants harvested at 1 week. Expression is found in recombinants that form prostate (UGM + UGE and UGM + BLE) but not in those that form bladder (BLM + UGE and BLM + BLE). Arrows in *C* and *E* indicate bladder-like structures that do not express *Nkx3.1*. (*F–I*) *Nkx3.1* expression in tissue recombinants of UGM with wild-type BLE (WT BLE) vs. UGM with BLE from *Tfm* mice (*Tfm* BLE), at 2 and 4 weeks of growth. (*B–I*) Scale bars, 50 μm.

appropriate combinations will give rise to prostate, identified by ductal histology and the production of characteristic secretory proteins, where different combinations will give rise to bladder or other tissues (Cunha et al. 1987; Cunha 1994). In particular, several nonprostatic epithelia (such as bladder epithelium) will form prostate when combined with the appropriate mesenchyme (such as urogenital sinus mesenchyme).

To ask whether *Nkx3.1* is expressed during the acquisition of prostate identity by epithelial tissues that do not form prostate in vivo, we performed tissue recombi-

nations with epithelial and mesenchymal components from embryonic urogenital sinus and neonatal bladder (Fig. 3B–E). *Nkx3.1* expression was only detected in tissue recombinants containing urogenital sinus mesenchyme, which induces prostate formation, but not in the tissue recombinants prepared with bladder mesenchyme, which induces bladder. *Nkx3.1* was expressed at early stages of prostate formation in the tissue recombinants, when the prostatic ducts have just begun to form. Importantly, *Nkx3.1* expression was induced in bladder epithelium combined with urogenital sinus mesenchyme (Fig. 3D). Conversely, expression was not detectable in tissue recombinants of urogenital sinus epithelium with bladder mesenchyme (Fig. 3C), indicating that expression was lost in response to inappropriate mesenchyme. Thus, *Nkx3.1* is an early and specific marker of prostate identity in tissue recombinants.

The time course of recombinant growth parallels aspects of prostate development in vivo, as tissue recombinants grown for an extended period resemble mature prostate and produce secretory proteins (Donjacour and Cunha 1993). This maturation process requires androgen receptor signaling in the epithelium (Donjacour and Cunha 1993), as shown using *Testicular feminization* (*Tfm*) mutant mice, which lack functional androgen receptors (Lyons and Hawkes 1970). Tissue recombinants prepared with *Tfm* epithelium initially form prostatic-like ducts, but subsequently fail to mature and express secretory proteins. Consequently, we examined the relationship of *Nkx3.1* expression and androgen receptor signaling, using prostatic tissue recombinants with normal (UGM + WT BLE) or defective (UGM + *Tfm* BLE) epithelial androgen receptor signaling (Fig. 3F–I). At early stages of growth (1 and 2 weeks), *Nkx3.1* expression was found in both UGM + WT BLE and UGM + *Tfm* BLE tissue recombinants (Fig. 3F,H; data not shown), although at lower levels in the latter. At 4 weeks of growth, however, *Nkx3.1* expression was greatly reduced or eliminated in UGM + *Tfm* BLE tissue recombinants (Fig. 3G,I). These findings indicate that epithelial androgen receptors are required for maintenance of *Nkx3.1* expression and suggest that *Nkx3.1* expression is associated with mature functional prostate.

Targeted disruption of Nkx3.1 *results in a defect in prostate ductal morphogenesis*

To examine the function of *Nkx3.1*, we performed targeted gene disruption via homologous recombination in embryonic stem (ES) cells. We constructed a positive–negative replacement vector that would delete the homeodomain and carboxy-terminal protein sequences, and thus should generate a null mutation (Fig. 4A). Following germ-line transmission of the targeted allele, we intercrossed heterozygous animals to recover viable and healthy homozygous adults that lack *Nkx3.1* expression (Fig. 4B–E). Although *Nkx3.1* homozygotes are fertile, homozygous males have difficulty forming copulatory plugs with advancing age (R. Bhatia-Gaur, C.Abate-Shen, and M.M. Shen, unpubl.)

Analysis of homozygous mutant adult males revealed that their urogenital systems were complete, but displayed morphological defects in the prostate gland and the BUG (Fig. 4F–H). Although all three prostatic lobes were present in the homozygous males, the number of prostatic ducts appeared fewer than in wild type. Quantitative analysis of ductal tip number in adult prostatic lobes demonstrated a significant reduction to 60%–75% of wild type (Fig. 4I,J). Moreover, this reduction in ductal tip number is evident as early as 10–11 days of age (data not shown), when ductal branching is nearly complete, but pubertal growth has not yet begun (Sugimura et al. 1986). In contrast, the overall sizes and wet weights of the prostatic lobes in the homozygotes were similar to wild type (data not shown). Because there is reduced ductal branching without an accompanying decrease in overall size, these data indicate reduced ductal complexity in *Nkx3.1* mutant prostates.

Nkx3.1 *mutant mice display altered production of prostatic secretory proteins*

During adult life, the primary function of the prostate is to contribute secretory proteins to the seminal fluid. In our analysis, we observed that the anterior prostate of *Nkx3.1* homozygotes frequently displayed a transparent appearance (Fig. 4G), suggesting defects in protein secretion relative to the wild-type gland, which is typically opaque. Consequently, we examined production of prostatic secretory proteins from wild-type, heterozygous, and homozygous mutant mice by SDS–polyacrylamide gel electrophoresis (Fig. 4L).

We found that several major prostatic secretory proteins were greatly reduced or eliminated in homozygous *Nkx3.1* males (Fig. 4L, asterisks); no differences were observed in seminal vesicles used as a negative control. We routinely observed that the prostatic lobes of homozygotes contained significantly less secretory material by volume and concentration than wild-type littermate controls; for example, the total protein concentration of ventral prostate secretions in homozygotes was 2.6-fold reduced relative to wild type ($n = 6$). To determine the identity of a major altered protein band, we performed microsequencing on a protein that is abundant in wild-type ventral prostate secretions but reduced or eliminated in *Nkx3.1* heterozygous and homozygous ventral prostate secretions (Fig. 4L; VP band marked with arrowhead). Sequence analyses revealed that this protein corresponds to the prostatic spermine-binding protein (SBP) precursor (R. Bhatia-Gaur, W. Lane, and C. Abate-Shen, unpubl.), which is the major secretory component of the ventral prostate (Mills et al. 1987). These findings demonstrate a profound defect in the production of specific prostatic secretory proteins in *Nkx3.1* mutant mice.

The BUG of Nkx3.1 *mutants displays altered cellular differentiation*

In *Nkx3.1* mutant males, the BUGs displayed a marked reduction in overall size and cellular composition rela-

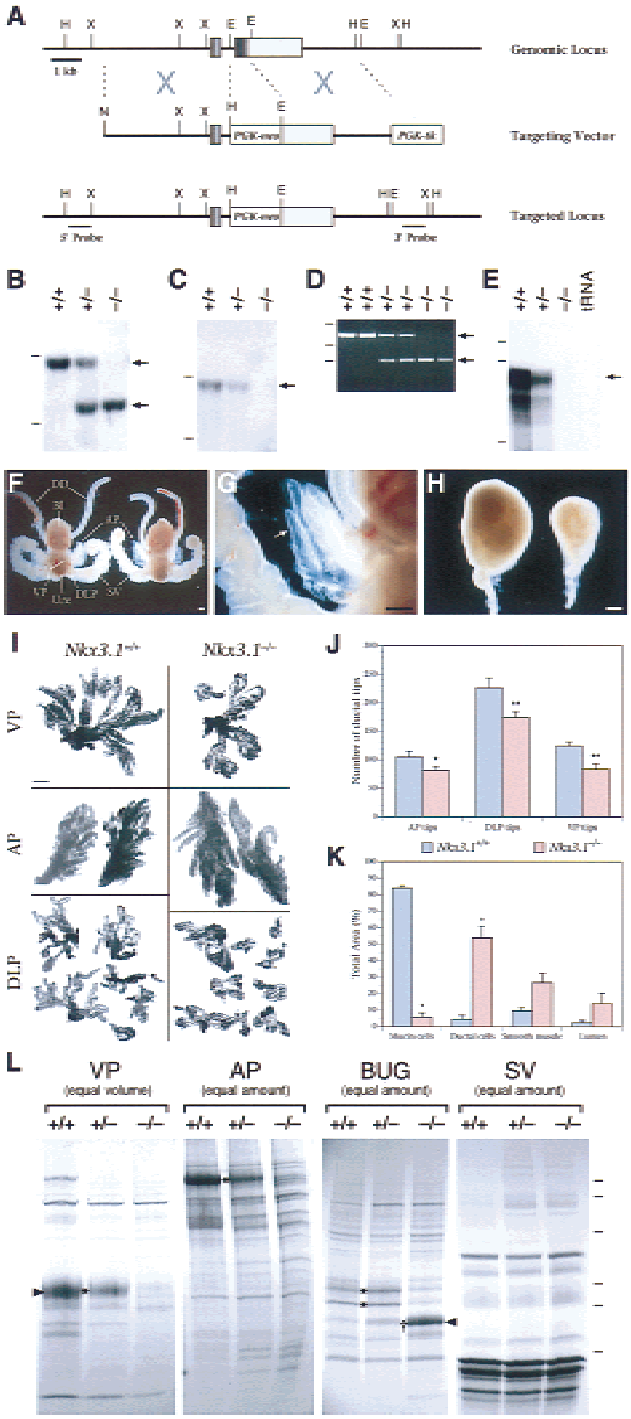

Figure 4. Analysis of *Nkx3.1* mutant mice. (*A–E*) Targeted disruption of *Nkx3.1*. (*A*) Strategy for gene disruption. The *Nkx3.1* locus comprises two exons (gray boxes), with the coding region (medium gray) contained in both exons and the homeobox in the second exon (dark gray). Homologous recombination with the targeting vector deletes most of the coding region, including the homeobox. The positions of the 5′- and 3′-flanking probes used for Southern blot analysis are shown. (E) *Eco*RI; (H) *Hind*III; (N) *Not*I; (X) *Xba*I. (*B*) Southern blot analysis of genomic DNA using the 5′- flanking probe, showing recovery of wild-type (+/+), heterozygous (+/−), and homozygous (−/−) adult mice. This probe detects a 9-kb *Hin*dIII wild-type fragment and a 6-kb fragment from the targeted allele (arrows). (*C*) Southern blot analysis using an internal probe containing the homeobox, confirming its deletion in *Nkx3.1* homozygotes. This probe detects a 9-kb *Hin*dIII wild-type fragment (arrow) and does not hybridize to the targeted allele. Dashes in *B* and *C* indicate positions of markers at 10 and 5 kb. (*D*) PCR analysis of genomic DNA from wild-type, heterozygous, and homozygous adult mice. Primers (described in Materials and Methods) amplify a 707-bp fragment from wild-type genomic DNA and a 232-bp fragment from the targeted allele (arrows). Dashes indicate positions of markers at 1018, 506, and 220 bp. (*E*) Ribonuclease protection analysis of total RNA from the APs of 8-week-old mice, using an *Nkx3.1* antisense riboprobe corresponding to the homeobox. Dashes indicate positions of markers at 220, 201, and 154 nucleotides. (*F–H*) Morphology of male urogenital tissues from wild-type and *Nkx3.1* mutant littermates. (*F*) Urogenital systems from wild-type (*left*) and *Nkx3.1* homozygote (*right*) at 8 weeks of age, showing positions of prostatic lobes (AP, DLP, VP), bladder (Bl), ductus deferens (DD), urethra (Ure), and seminal vesicles (SV). (*G*) Higher-power view of the mutant anterior prostate shown in *E*, with semitransparent ducts (arrow). (*H*) BUGs from wild-type (*left*) and *Nkx3.1* homozygote (*right*) at 6 weeks of age. Scale bars in *F–H*, 0.5 mm. (*I*) Microdissected prostatic lobes from wild-type and *Nkx3.1* homozygous mice at 12 weeks of age. Scale bar, 1.0 mm. (*J*) Quantitation of ductal tips, analyzed as in *H*. The mean number of ductal tips was significantly smaller in each of the mutant prostatic lobes, at $P < 0.1$ (*) or $P < 0.05$ (**). (*K*) Quantitation of the histological composition of the wild-type and *Nkx3.1* mutant BUGs. The total area analyzed was 6.1×10^7 μm^2 for wild-type glands and 2.5×10^7 μm^2 for mutant glands; significant differences from the wild-type ($P < 0.05$) are indicated (*). In *J* and *K*, error bars represent standard error of the mean (S.E.M.). (*L*) Analysis of secretory proteins from VP and AP prostatic lobes, BUG, and SV. Protein secretions were collected from tissues of 8-week-old male mice and resolved on a 10%–20% SDS–polyacrylamide gradient gel. (Equal volume) Lanes contain 4 μl of secretory material; (equal amount) lanes contain 10 μg of total protein. Asterisks (*) indicate proteins that are decreased in −/− mice; (†) a protein increased in homozygotes. Arrowheads indicate the protein bands analyzed by microsequencing. Dashes at *right* mark the positions of molecular mass standards at 102, 81, 46.9, 32.7, 30.2, and 24 kD.

tive to wild-type controls (Fig. 4H,K; Fig. 5A–D). In particular, these glands were dramatically reduced in wet weight compared to wild type [14.4 ± 2.4 mg (n = 10) vs. 32.2 ± 2.1 mg (n = 6)]. Furthermore, whereas the wild-type (and heterozygous) BUGs are primarily composed of mucin-producing cells, the homozygous mutant glands show a dramatic loss of these cells, and are instead composed primarily of ductal cells (Fig. 5A–D). Quantitative analysis demonstrated a 15-fold reduction of mucin cells in the homozygote relative to the wild type, and a corresponding 11-fold increase in ductal cells (Fig. 4K). The abundant ductal cells in *Nkx3.1* mutants resemble a minor constituent of the wild-type BUG that is primarily found near the neck of the gland (A.A. Donjacour, R.D. Cardiff, G.R. Cunha, C. Abate-Shen, and M.M. Shen, unpubl.).

Secretory protein production was also significantly altered in the *Nkx3.1* homozygous BUG. In particular, we observed a novel protein species in the secretions from mutant glands (Fig. 4L, dagger), as well as reduced levels

of wild-type secretory proteins (Fig. 4L, asterisks). Microsequence analysis of this novel secretory protein (R. Bhatia-Gaur, W. Lane, and C. Abate-Shen, unpubl.) revealed that it corresponds to p20, an abundant component of salivary gland secretion that is related to the rat common salivary protein 1 (CSP1) (Girard et al. 1993;

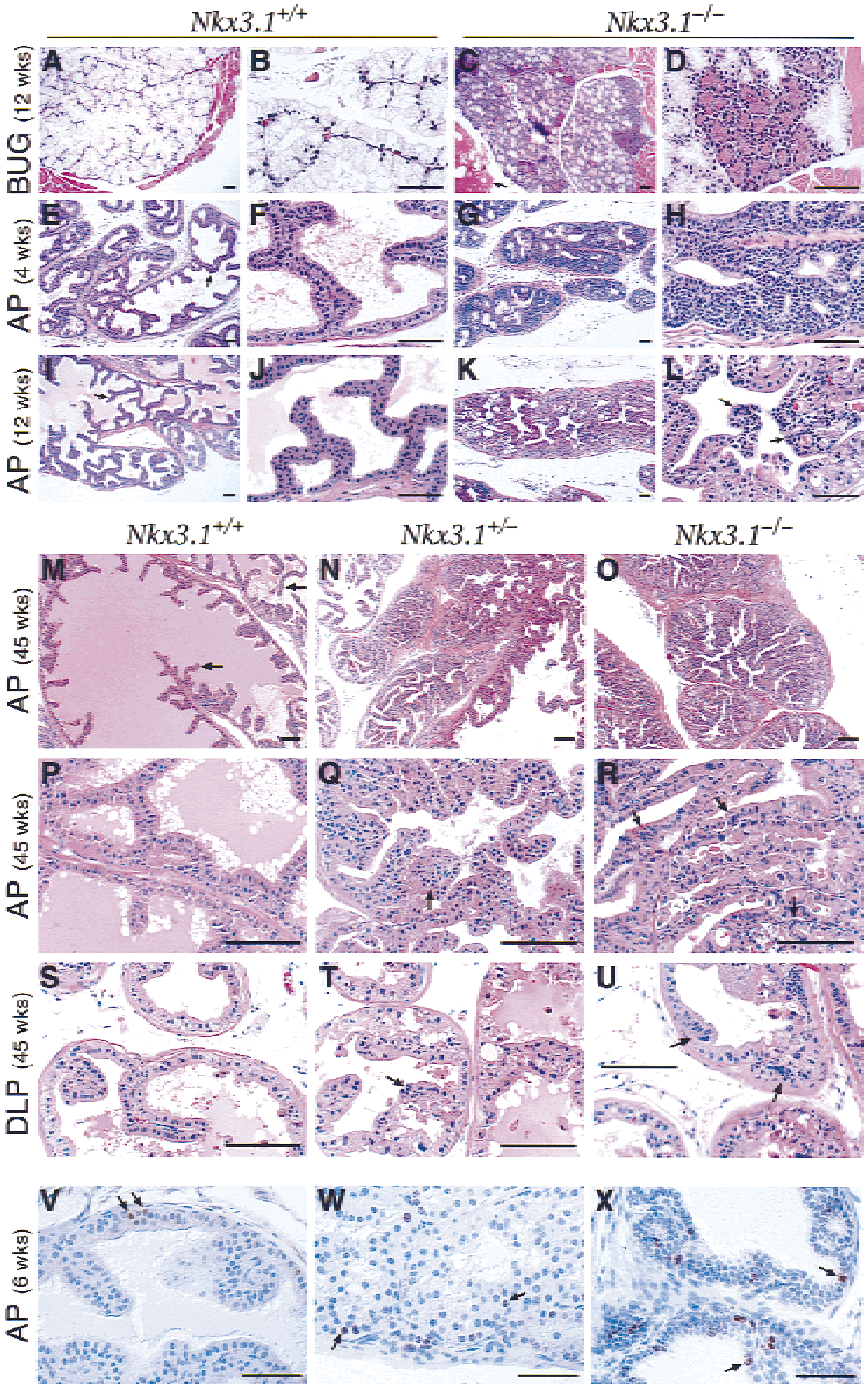

Figure 5. (*See facing page for legend.*)

Bekhor et al. 1994). Taken together, these observations demonstrate that *Nkx3.1* is essential for the appropriate differentiation and secretory function of the BUG, and suggest that its loss converts a mucin-producing tissue into a ductal tissue.

Nkx3.1 *homozygous and heterozygous mice display prostatic epithelial hyperplasia and dysplasia*

The most notable phenotype of the *Nkx3.1* mutant prostatic lobes is the histological appearance of epithelial hyperplasia and dysplasia, which becomes increasingly severe with advancing age. In wild-type adult mice, the prostate contains a simple tall columnar epithelium, with each prostatic lobe displaying a characteristic histological appearance. In particular, the epithelium of the anterior prostate forms distinct papillary tufts that are apparent by 4 weeks of age (during puberty) and continue to form throughout adult life (Fig. 5E,F,I,J,M,P). In contrast, as early as 4 weeks of age, the anterior prostate of homozygous *Nkx3.1* mutants contains a multilayered hyperplastic epithelium with relatively normal nuclear morphology (Fig. 5G,H). By 12 weeks of age, the anterior prostate epithelium of homozygotes also contains dysplastic regions of epithelium showing variation in nuclear size and shape as well as abnormal mitotic figures, with a corresponding loss of lumenal space and secretory material (Fig. 5K,L). This hyperplastic growth may account for why prostatic lobes of *Nkx3.1* mutants have a reduced number of ducts yet are not reduced in wet weight (Fig. 4I,J; data not shown).

At 1 year of age, which represents the oldest mice analyzed to date, the anterior prostate of homozygotes displays extensive hyperplastic epithelium with focal areas that are severely dysplastic (Fig. 5O,R), although no overt tumors have yet been observed. Notably, a similar but less severe hyperplastic and dysplastic epithelium is observed in heterozygous *Nkx3.1* mutants, indicating haploinsufficiency for this phenotype (Fig. 5N,Q). Furthermore, at 1 year of age, the dorsolateral prostate of homozygotes displays mild hyperplasia and severe dysplasia (Fig. 5U); the heterozygous dorsolateral prostates are also affected, though less severely (Fig. 5T). Interestingly, no histopathological defect has yet been observed in the ventral prostate (data not shown). Analysis of cellular proliferation using an anti-Ki67 antibody in an experimental cohort at 6 weeks of age demonstrated a 5.8-fold increase in proliferating cells in the homozygous anterior prostate and a 4.5-fold increase in the heterozygous, as compared with wild type (Fig. 5V–X). These data demonstrate epithelial hyperproliferation in *Nkx3.1* homozygotes and heterozygotes, indicating that the observed cytological and morphological changes model a preneoplastic condition.

Discussion

Our analysis of *Nkx3.1* provides a molecular link between the mechanisms that control normal prostate differentiation and those that lead to deregulated epithelial proliferation during prostate carcinogenesis. Thus, we have shown that *Nkx3.1* is essential for normal morphogenesis and function of the prostate, whereas its inactivation leads to prostatic epithelial hyperplasia and dysplasia that model a preneoplastic condition (Fig. 6). Taken together with the observation that human *NKX3.1* maps to the minimal region of chromosome 8p21 that undergoes loss of heterozygosity in prostate tumors (He et al. 1997; Voeller et al. 1997), we propose that *NKX3.1* maintains the differentiated state of normal prostate, whereas its loss represents a predisposing event for prostate carcinogenesis.

Nkx3.1 *expression defines early events in prostate formation*

Little is known about the early events of prostate formation and the molecular pathways involved in this process. Until now, it has been presumed that signals from the urogenital sinus mesenchyme are solely responsible for inducing the epithelium to form prostatic buds. However, we have found that *Nkx3.1* expression marks prospective prostate epithelium 2 days prior to the appearance of prostatic buds, suggesting that the urogenital sinus epithelium has a differential capacity to respond to mesenchymal signals before overt morphogenesis oc-

Figure 5. Histology of *Nkx3.1* mutant mice. (*A–U*) H&E staining of paraffin sections of BUG, AP, and DLP in wild-type (*Nkx3.1*$^{+/+}$), heterozygous (*Nkx3.1*$^{+/-}$), and homozygous (*Nkx3.1*$^{-/-}$) mice at 4, 12, and 45 weeks of age. (*A–D*) At 12 weeks of age, the wild-type BUG (*A*,*B*) contains differentiated mucin-producing cells; while the homozygous gland (*C*,*D*) largely contains cells with ductal morphology. (*E–H*) At 4 weeks of age, the wild-type anterior prostate (*E*,*F*) contains immature columnar epithelial cells arranged in characteristic papillary tufts (arrow); the homozygous anterior prostate (*G*,*H*) contains a multilayered hyperplastic epithelium, with little lumenal space. (*I–L*) At 12 weeks of age, the wild-type anterior prostate (*I*,*J*) contains differentiated columnar epithelial cells with lumenal spaces filled with secretions (lightly staining eosinophilic material). The homozygous AP (*K*,*L*) contains hyperplastic epithelium with mildly dysplastic regions (arrows), and little secretory material. (*M–R*) At 45 weeks of age, the wild-type AP (*M*,*P*) contains tall columnar epithelium arranged in papillary tufts (arrow), the heterozygous AP (*N*,*Q*) contains hyperplastic epithelium with mildly dysplastic regions (arrow) and reduced lumenal space and secretory protein, and the homozygous AP (*O*,*R*) contains severely hyperplastic epithelium and regions of dysplasia (arrows). (*S–U*) At 45 weeks of age, the wild-type DLP (*S*) contains columnar epithelium and lumenal secretions, the heterozygous DLP (*T*) contains areas of mild dysplasia (arrow), and the homozygous DLP (*U*) contains severely dysplastic epithelium (arrows). (*V–X*) Ki67 immunoreactivity in the anterior prostates of wild-type (*V*), heterozygous (*W*), and homozygous (*X*) *Nkx3.1* mice at 6 weeks of age. Arrows indicate Ki67-labeled nuclei. In total, 55 Ki67-labeled nuclei were observed out of 3767 total nuclei (1.5%) in wild type; 207 of 2991 (6.9%) in heterozygotes; and 315 of 3573 (8.8%) in homozygotes. (*A–L* and *V–X*) Scale bars, 50 μm; (*M–U*) scale bars, 100 μm.

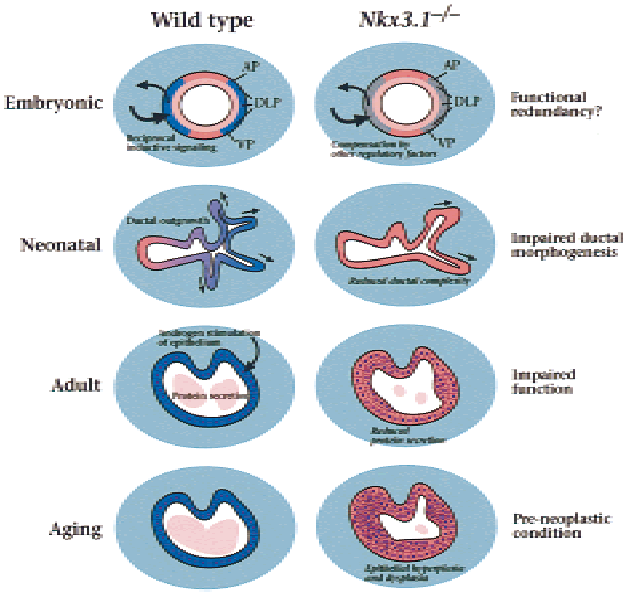

Figure 6. Model for *Nkx3.1* activities in prostate development, maturation, and carcinogenesis. The model is described in the text; expression of *Nkx3.1* is shown in blue.

curs. In particular, the parentheses expression pattern of *Nkx3.1* defines zones of urogenital sinus epithelium, such that the dorsal boundaries correspond to the prospective anterior prostate, the intermediate regions to the dorsolateral prostate, and the ventral boundaries to the ventral prostate (Fig. 2, cf. G with H and E; Fig. 6). Thus, we speculate that *Nkx3.1* expression reveals a prepatterning of the urogenital sinus epithelium into distinct prostatic and nonprostatic regions.

Although *Nkx3.1* is the earliest known differentiation marker of the prostate epithelium, it must cooperate with other regulatory genes, as its loss of function does not result in complete failure of prostate formation (Fig. 6). Among other putative transcription factors, posterior members of the *HoxD* cluster are known to be expressed in adult prostate and are required for correct prostate morphogenesis (Oefelein et al. 1996; Podlasek et al. 1997). Among secreted signaling molecules, *Sonic hedgehog* (*Shh*) is known to regulate *Nkx3.1* expression during somite formation (Kos et al. 1998). In preliminary studies, we have observed *Shh* expression in urogenital sinus epithelium prior to prostatic bud formation (J. Bush, C. Abate-Shen and M.M. Shen, unpubl.). Our description of *Nkx3.1* expression provides a foundation for future studies to identify other regulatory components responsible for prostate formation.

Roles for Nkx3.1 *in prostate differentiation and function*

Nkx3.1 expression is associated with all aspects of embryonic prostate development, neonatal differentiation, and adult function (Fig. 6). In many respects, the expression pattern of *Nkx3.1* and the phenotype of mutant mice are analogous to those of other vertebrate *Nkx* homeobox genes. For example, *Nkx2.5* is expressed in precardiac mesoderm and in the developing heart, and null mutation results in defects in cardiac looping morphogenesis and myogenesis (Lints et al. 1993; Lyons et al. 1995). Similarly, *Nkx2.1* is expressed during lung development, and targeted disruption leads to severe defects in bronchial branching (Kimura et al. 1996). These *Nkx* genes are expressed in highly restricted patterns during early stages of tissue specification and subsequent morphogenesis, as is observed for *Nkx3.1* expression in prospective as well as differentiating prostate epithelium. Furthermore, mutations in *Nkx* genes result in defects in morphogenesis as well as in cellular differentiation, analogous to the defects in ductal branching and protein secretion found in *Nkx3.1* mutants. Thus, like other *Nkx* homeobox genes, *Nkx3.1* plays an essential role in organogenesis.

In addition to its role in prostate development, *Nkx3.1* has a distinct and unique function in the BUG, as *Nkx3.1* mutants display a dramatic loss of mucin-producing cells and a corresponding increase of ductal cells. Despite their similar embryological origins, the prostate gland and BUG are morphologically, histologically, and functionally distinct. Whereas the prostatic lobes are comprised of tall columnar epithelium surrounded by smooth muscle stroma, the BUG primarily consists of mucin-producing cells within a skeletal muscle capsule. Notably, the epithelium of the prostate, but not that of the BUG, is highly susceptible to hyperplastic growth and carcinogenesis. Accordingly, loss of *Nkx3.1* function results in a profound alteration in cellular composition but does not lead to hyperplastic growth of the bulbourethral epithelium.

Prostate organogenesis is intimately associated with a requirement for androgen signaling from the earliest stages of prostate formation through mature function. During embryogenesis, mesenchymal androgen receptors are required for prostate formation (Cunha et al. 1987), whereas during adulthood, epithelial androgen receptors are required for secretory protein production (Donjacour and Cunha 1993). Our results indicate that androgen receptor signaling in the prostate epithelium is not required for the initiation of *Nkx3.1* expression, as its expression precedes the appearance of functional epithelial androgen receptors (Takeda and Chang 1991). However, the absence of *Nkx3.1* expression in the female urogenital system implies that mesenchymal androgen receptors are indirectly required for initiation of its expression. Furthermore, maintained expression of *Nkx3.1* requires androgen receptor signaling, as shown in vivo and in cultured cells (Bieberich et al. 1996; He et al. 1997; Sciavolino et al. 1997; Prescott et al. 1998). Consistent with these observations, *Nkx3.1* is expressed at early, but not later, stages in tissue recombinants lacking epithelial androgen receptors (UGM + *Tfm* BLE). These tissue recombinants do not produce secretory proteins, further underscoring the relationship between *Nkx3.1* expression and secretory protein production. Because *Nkx3.1* encodes a putative transcription factor, it may

regulate the expression of specific secretory proteins in response to androgen receptor signaling.

Potential role for Nkx3.1 *in prostate carcinogenesis*

In addition to its chromosomal localization to a prostate cancer hot spot, several lines of evidence implicate *NKX3.1* as a candidate prostate tumor suppressor gene. Notably, we have shown that *Nkx3.1* mutant mice display epithelial hyperplasia and dysplasia, modeling a preneoplastic condition (Fig. 6). This epithelial hyperplasia and dysplasia mimic the time course of prostate cancer progression in human patients, which occurs as a consequence of aging. Furthermore, we have observed that overexpression of human or murine *NKX3.1* suppresses growth and tumorigenicity of prostate carcinoma cells in culture (R. Bhatia-Gaur, M. Kim, M.M. Shen, and C. Abate-Shen, unpubl.). At present, there is no evidence for mutations of the *NKX3.1* coding region in human prostate tumors (Voeller et al. 1997). However, our analysis of *Nkx3.1* heterozygous mice demonstrates haploinsufficiency for the epithelial hyperplasia and dysplasia phenotype. Therefore, loss of a single *NKX3.1* allele may be sufficient to promote prostate carcinogenesis in humans. Haploinsufficiency of other tumor suppressor genes has been implicated in cancer progression (Fero et al. 1998). Because candidate tumor suppressor genes are often not mutated in prostate tumor specimens, haploinsufficiency may be of general significance in prostate cancer.

Although many homeobox genes have been implicated in carcinogenesis, *Nkx3.1* is unusual in that it is a candidate tumor suppressor gene, rather than an oncogene. We propose that loss of human *NKX3.1* is an early event in prostate carcinogenesis that results in a preneoplastic condition, whereas subsequent genetic events promote progression to overt carcinoma. Candidate genetic events that may act in concert with loss of *NKX3.1* include loss of *MXI1* and/or *PTEN*, as the corresponding mutant mice display prostatic epithelial hyperplasia and dysplasia, with no overt neoplastic transformation (Di Crisofano et al. 1998; Schreiber-Agus et al. 1998). Thus, the *Nkx3.1* mutant mice should serve as an excellent model for recapitulating the molecular events of prostate cancer initiation and for defining downstream genetic events in prostate cancer progression.

Materials and methods

Expression analysis

Ribonuclease protection analyses were performed on total RNA isolated from individually dissected prostatic lobes or other tissues from 8-week-old male virgin Swiss–Webster mice (Taconic), as described (Shen and Leder 1992). The antisense riboprobes correspond to a 286 bp cDNA fragment spanning exons 1 and 2 (Fig. 1C) or a 187-bp fragment from exon 2 that includes the homeobox (Fig. 4E). Quantitation was performed using a PhosphorImager (Molecular Dynamics), and the *Nkx3.1* signal was normalized to the L32 ribosomal protein internal control probe (Shen and Leder 1992). Note that the previously reported expression of *Nkx3.1* in seminal vesicle (Sciavolino et al. 1997) was likely due to contamination by anterior prostate. For section in situ hybridization, mouse embryos were obtained at 14.5–17.5 dpc (where day 0.5 is defined as noon of the day of the copulatory plug) and sexed by PCR using primers for the *Sry* gene (Hogan et al. 1994). Neonatal prostatic lobes and other urogenital tissues were dissected individually at P0, P8, and P18. In situ hybridization was carried out as described (Sciavolino et al. 1997), with at least two and usually four specimens from each stage, using a digoxigenin-labeled riboprobe corresponding to a 1-kb *Eco*RI fragment of the *Nkx3.1* cDNA.

For tissue recombination studies, rat urogenital sinus mesenchyme (17.5 dpc) and mouse urogenital sinus mesenchyme and epithelium (15.5 dpc) were obtained as described (Cunha and Donjacour 1987; Higgins et al. 1989). Bladder mesenchyme and epithelium were obtained (Cunha and Donjacour 1987) from adult or P0 wild-type mice, or from homozygous *Tfm* mice (Lyons and Hawkes 1970). Tissue recombinants were grafted into adult male *nude* mouse hosts for 1, 2, or 4 weeks (Cunha and Donjacour 1987). Upon harvesting, tissues were processed for in situ hybridization and histology.

Gene targeting

Nkx3.1 genomic clones were isolated from a λFIXII library constructed from 129Sv/J genomic DNA (Stratagene). The targeting vector was constructed in p*PNT* (Tybulewicz et al. 1991), using a 4.1-kb *Eco*RI fragment as the 3′ flank, and a 4.5-kb *Not*I–*Eco*RI fragment as the 5′ flank. The linearized construct was electroporated into CJ7 ES cells (Swiatek and Gridley 1993), and targeted clones were obtained at a frequency of 4% (3/85). Chimeric males obtained following blastocyst injection were bred with C57Bl/6J females (Jackson Laboratories), and germ-line transmission was obtained from a single targeted ES clone. The targeted allele has been maintained on a hybrid 129/SvImJ and C57Bl/6J strain background, as well as on an inbred 129/SvImJ background. Results shown were obtained using mice in the hybrid background; the prostate phenotype appears similar in the 129/SvImJ inbred background (R. Bhatia-Gaur, C. Abate-Shen, and M.M. Shen, unpubl.).

Genotyping of the *Nkx3.1* mutant mice was performed by Southern blot analysis and PCR. The sequence of the primers used for PCR analysis were 5′-GTCTTGGAGAAGAACTCACCATTG-3′ (wild-type *Nkx3.1* forward), 5′-TTCCACATACACTTCATTCTCAGT-3′ (mutated forward), and 5′-GCCAACCTGCCTCAATCACTAAGG-3′ (wild-type and mutated reverse).

Analysis of the Nkx3.1 *mutant phenotype*

Analyses were performed using virgin male mice from P0 through 12 months of age; experimental cohorts were wild-type, heterozygous, and homozygous littermates (Table 1). For analysis of wet weights and ductal tips, male reproductive organs were dissected and bilateral organ pairs weighed (Sugimura et al. 1986; Donjacour et al. 1998). The gross morphology and wet weights of the epididymides, ductus deferens, ampullary glands, seminal vesicles, preputial glands, and testes of adult homozygous mutants were identical to those of wild type (data not shown). Prostatic ductal tips were traced and counted from digitized images. Organ weights and ductal tips were compared by Student's *t*-test. To determine the proportion of cell types in the BUG, random images were captured from hematoxylin-and-eosin (H&E) stained sections, and areas were calculated using NIH Image software. We note that the lack of morphological or histological (see below) defects in the testes or in androgen-depen-

Table 1. *Number of mice analyzed*

Method	Age	+/+	+/−	−/−
Prostate ductal tip counting	1–2 days	7	6	9
	10–12 days	2	5	7
	12 weeks	6	16	10
BUG composition	12 weeks	5	0	5
Protein secretion	8 weeks	4	1	4
	12 weeks	1	1	1
	20 weeks	1	0	1
	11–12 months	2	2	2
Histological analysis	8 days	1	1	1
	3–4 weeks	2	3	2
	8 weeks	6	6	6
	12 weeks	4	6	4
	5 months	1	2	2
	11–12 months	4	4	4

dent tissues, such as the ductus deferens and seminal vesicle, indicates that the reduced number of prostatic ductal tips is not due to decreased androgen levels; however, a very subtle defect in androgen production cannot be excluded.

For analysis of secretory proteins from dissected AP, BUG, and seminal vesicle, secretions were collected in PBS containing 1 mM PMSF by gentle squeezing (Donjacour and Cunha 1993). Dorsolateral and ventral prostate secretions were recovered by scoring of the ducts, followed by centrifugation in PBS with 1 mM PMSF. Secretory proteins were resolved on 10%–20% gradient SDS–polyacrylamide gels (Bio-Rad), followed by visualization with Coomassie Brilliant blue. For protein sequence analysis, individual protein bands were isolated from SDS-Polyacrylamide gels, and analysis performed at the Harvard Microchemistry Facility by microcapillary reverse-phase HPLC tandem mass spectrometry (μLC/MS/MS) on a Finnigan LCQ quadrupole ion trap mass spectrometer.

For histological analysis, dissected tissues were fixed in OmniFix 2000 (Aaron Medical Industries, St. Petersburg, FL), and processed for H&E staining. For all cohorts, the prostatic lobes, seminal vesicles, ductus deferens, epididymides, and testes were examined. For one cohort (8 weeks of age), the lungs, brain, liver, kidney, heart, salivary glands, and intestines were also examined and found to have normal histology (data not shown). The primary histological analysis was performed on a nonblinded basis (by R.D. Cardiff); one of us (M.M. Shen) independently reviewed the histological data on a blinded basis, reaching similar conclusions. Cellular proliferation was analyzed in mice at 6 and 20 weeks of age by immunohistochemical staining of formalin-fixed tissues using a rabbit polyclonal anti-Ki67 antibody (Novocastra Laboratories). Ki67-labeled nuclei were quantitated by counting ~3000 hematoxylin-stained nuclei from high-power microscopic fields.

Acknowledgments

We thank Whitney Banach and Sandy Price for assistance with animal husbandry, Judy Walls for histology, Yu-Ting Yan for advice on design of the gene targeting vector, and Lu Yang for advice on in situ hybridization. Protein microsequencing was performed by William S. Lane and colleagues at the Microchemistry Facility at Harvard University. We also thank Andy McMahon, Frank Rauscher III, Danny Reinberg, Nicole Schreiber-Agus, and Cliff Tabin for comments on the manuscript, and members of the Abate-Shen, Shen, and Cunha laboratories for helpful discussions. This work was supported by National Institutes of Health grant CA76501 to C.A.-S.; U.S. Army Prostate Cancer Research Program grant DAMD17-98-1-8532 to M.M.S.; NIH grants DK52721, CA59831, DK51101, DK51397, DK45861, CA64872, DK52708, and DK47517 to G.R.C.; NIH grants NS36437 and HD34883 to T.G.; NIH grant CA34196 to the Jackson Laboratory; and NIH training grant T32-MH019957 to R.B.-G.

The publication costs of this article were defrayed in part by payment of page charges. This article must therefore be hereby marked 'advertisement' in accordance with 18 USC section 1734 solely to indicate this fact.

References

Bekhor, I., Y. Wen, S. Shi, C.H. Hsieh, P.A. Denny, and P.C. Denny. 1994. cDNA cloning, sequencing and in situ localization of a transcript specific to both sublingual demilune cells and parotid intercalated duct cells in mouse salivary glands. *Arch. Oral Biol.* **39:** 1011–1022.

Bergerheim, U.S.R., K. Kunimi, V.P. Collins, and P. Ekman. 1991. Deletion mapping of chromosomes 8, 10, and 16 in human prostatic carcinoma. *Genes Chromosomes Cancer* **3:** 215–220.

Bieberich, C.J., K. Fujita, W.W. He, and G. Jay. 1996. Prostate-specific and androgen-dependent expression of a novel homeobox gene. *J. Biol. Chem.* **271:** 31779–31782.

Bova, G.S., B.S. Carter, M.J.G. Bussemakers, M. Emi, Y. Fujiwara, N. Kyprianou, S.C. Jacobs, J.C. Robinson, J.I. Epstein, P.C. Walsh, and W.B. Isaacs. 1993. Homozygous deletion and frequent allelic loss of chromosome 8p22 loci in human prostate cancer. *Cancer Res.* **53:** 3869–3873.

Cher, M.L., G.S. Bova, D.H. Moore, E.J. Small, P.R. Carroll, S.S. Pin, J.I. Epstein, W.B. Isaacs, and R.H. Jensen. 1996. Genetic alterations in untreated metastases and androgen-independent prostate cancer detected by comparative genomic hybridization and allelotyping. *Cancer Res.* **56:** 3091–3102.

Coffey, D.S. 1992. Prostate cancer: An overview of an increasing dilemma. *Cancer* **71:** 880–886.

Cooke, P.S., P.F. Young, and G.R. Cunha. 1987a. Androgen dependence of growth and epithelial morphogenesis in neonatal mouse bulbourethral glands. *Endocrinology* **121:** 2153–2160.

———. 1987b. A new model system for studying androgen-induced growth and morphogenesis in vitro: The bulbourethral gland. *Endocrinology* **121:** 2161–2170.

Cunha, G.R. 1994. Role of mesenchymal-epithelial interactions in normal and abnormal development of the mammary gland and prostate. *Cancer* **74:** 1030–1044.

Cunha, G.R. and A. Donjacour. 1987. Mesenchymal-epithelial interactions: Technical considerations. *Prog. Clin. Biol. Res.* **239:** 273–282.

Cunha, G.R., A.A. Donjacour, P.S. Cooke, S. Mee, R.M. Bigsby, S.J. Higgins, and Y. Sugimura. 1987. The endocrinology and developmental biology of the prostate. *Endocr. Rev.* **8:** 338–362.

Di Crisofano, A., B. Pesce, C. Cordon-Cardo, and P.P. Pandolfi. 1998. *Pten* is essential for embryonic development and tumour suppression. *Nat. Genet.* **19:** 348–355.

Donjacour, A.A. and G.R. Cunha. 1988. The effect of androgen deprivation on branching morphogenesis in the mouse prostate. *Dev. Biol.* **128:** 1–14.

———. 1993. Assessment of prostatic protein secretion in tissue recombinants made of urogenital sinus mesenchyme and

urothelium from normal or androgen-insensitive mice. *Endocrinology* **132:** 2342–2350.

Donjacour, A.A., A.A. Thomson, and G.R. Cunha. 1998. Enlargement of the ampullary gland and seminal vesicle but not the prostate in *int2/Fgf-3* transgenic mice. *Differentiation* **62:** 227–237.

Fero, M.L., E. Randel, K.E. Gurley, J.M. Roberts, and C.J. Kemp. 1998. The murine gene $p27^{Kip1}$ is haplo-insufficient for tumour suppression. *Nature* **396:** 177–180.

Girard, L.R., A.M. Castle, A.R. Hand, J.D. Castle, and L. Mirels. 1993. Characterization of common salivary protein 1, a product of rat submandibular, sublingual, and parotid glands. *J. Biol. Chem.* **268:** 26592–26601.

Hayward, S.W., G.R. Cunha, and R. Dahiya. 1996. Normal development and carcinogenesis of the prostate. A unifying hypothesis. *Ann. NY Acad. Sci.* **784:** 50–62.

He, W.W., P.J. Sciavolino, J. Wing, M. Augustus, P. Hudson, P.S. Meissner, R.T. Curtis, B.K. Shell, D.G. Bostwick, D.J. Tindall, E.P. Gelmann, C. Abate-Shen, and K.C. Carter. 1997. A novel human prostate-specific, androgen-regulated homeobox gene (NKX3.1) that maps to 8p21, a region frequently deleted in prostate cancer. *Genomics* **43:** 69–77.

Higgins, S.J., P. Young, J.R. Brody, and G.R. Cunha. 1989. Induction of functional cytodifferentiation in the epithelium of tissue recombinants. I. Homotypic seminal vesicle recombinants. *Development* **106:** 219–234.

Hogan, B., R. Beddington, F. Costantini, and E. Lacy. 1994. *Manipulating the mouse embryo.* Cold Spring Harbor Laboratory Press, Cold Spring Harbor, NY.

Kimura, S., Y. Hara, T. Pineau, P. Fernandez-Salguero, C.H. Fox, J.M. Ward, and F.J. Gonzalez. 1996. The *T/ebp* null mouse: Thyroid-specific enhancer-binding protein is essential for the organogenesis of the Thyroid, lung, ventral forebrain, and pituitary. *Genes & Dev.* **10:** 60–69.

Kos, L., C. Chiang, and K.A. Mahon. 1998. Mediolateral patterning of somites: Multiple axial signals, including *Sonic hedgehog*, regulate *Nkx-3.1* expression. *Mech. Dev.* **70:** 25–34.

Landis, S.H., T. Murray, S. Bolden, and P.A. Wingo. 1998. Cancer statistics. *CA– Cancer J. Clin.* **48:** 6–29.

Lints, T.J., L.M. Parsons, L. Hartley, I. Lyons, and R.P. Harvey. 1993. Nkx-2.5: A novel murine homeobox gene expressed in early heart progenitor cells and their myogenic descendants. *Development* **119:** 419–431.

Lyons, I., P.L. M., L. Hartley, R. Li, J.E. Andrews, L. Robb, and R.P. Harvey. 1995. Myogenic and morphogenetic defects in the heart tubes of murine embryos lacking the homeo box gene *Nkx2-5. Genes & Dev.* **9:** 1654–1666.

Lyons, M.F. and S.G. Hawkes. 1970. X-linked gene for testicular feminization in the mouse. *Nature* **227:** 1217–1219.

McNeal, J.E. 1978. Evolution of benign prostatic enlargement. *Invest. Urol.* **15:** 340–345.

Mills, J.S., M. Needham, T.C. Thompson, and M.G. Parker. 1987. Androgen-regulated expression of secretory protein synthesis in mouse ventral prostate. *Mol. Cell. Endocrinol.* **53:** 111–118.

Oefelein, M., C. Chin-Chance, and W. Bushman. 1996. Expression of the homeotic gene *Hox-d13* in the developing and adult mouse prostate. *J. Urol.* **155:** 342–346.

Podlasek, C.A., D. Duboule, and W. Bushman. 1997. Male accessory sex organ morphogenesis is altered by loss of function of *Hoxd-13. Dev. Dyn.* **208:** 454–465.

Prescott, J.L., L. Blok, and D.J. Tindall. 1998. Isolation and androgen regulation of the human homeobox cDNA, NKX3.1. *Prostate* **35:** 71–80.

Schreiber-Agus, N., Y. Meng, T. Hoang, H. Hou, Jr., K. Chen, R. Greenberg, C. Cordon-Cardo, H.W. Lee, and R.A. DePinho. 1998. Role of Mxi1 in ageing organ systems and the regulation of normal and neoplastic growth. *Nature* **393:** 483–487.

Sciavolino, P.J., E.W. Abrams, L. Yang, L.P. Austenberg, M.M. Shen, and C. Abate-Shen. 1997. Tissue-specific expression of murine *Nkx3.1* in the male urogenital system. *Dev. Dyn.* **209:** 127–138.

Shen, M.M. and P. Leder. 1992. Leukemia inhibitory factor is expressed by the preimplantation uterus and selectively blocks primitive ectoderm formation *in vitro. Proc. Natl. Acad. Sci.* **89:** 8240–8244.

Sugimura, Y., G.R. Cunha, and A.A. Donjacour. 1986. Morphogenesis of ductal networks in the mouse prostate. *Biol. Reprod.* **34:** 961–971.

Swiatek, P.J. and T. Gridley. 1993. Perinatal lethality and defects in hindbrain development in mice homozygous for a targeted mutation of the zinc finger gene *Krox-20. Genes & Dev.* **7:** 2071–2084.

Takeda, H. and C. Chang. 1991. Immunohistochemical and in-situ hybridization analysis of androgen receptor expression during the development of the mouse prostate gland. *J. Endocrinol.* **129:** 83–89.

Trapman, J., H.F. Sleddens, M.M. van der Weiden, W.J. Dinjens, J.J. Konig, F.H. Schroder, P.W. Faber, and F.T. Bosman. 1994. Loss of heterozygosity of chromosome 8 microsatellite loci implicates a candidate tumor suppressor gene between the loci *D8S87* and *D8S133* in human prostate cancer. *Cancer Res.* **54:** 6061–6064.

Treier, M., A.S. Gleiberman, S.M. O'Connell, D.P. Szeto, J.A. McMahon, A.P. McMahon, and M.G. Rosenfeld. 1998. Multistep signaling requirements for pituitary organogenesis *in vivo. Genes & Dev.* **12:** 1691–1704.

Tybulewicz, V.L., C.E. Crawford, P.K. Jackson, R.T. Bronson, and R.C. Mulligan. 1991. Neonatal lethality and lymphopenia in mice with a homozygous disruption of the c-*abl* proto-oncogene. *Cell* **65:** 1153–1163.

Vocke, C.D., R.O. Pozzatti, D.G. Bostwick, C.D. Florence, S.B. Jennings, S.E. Strup, P.H. Duray, L.A. Liotta, M.R. Emmert-Bucke, and W.M. Lineham. 1996. Analysis of 99 microdissected prostate carcinomas reveals a high frequency of allelic loss on chromosome 8p12-21. *Cancer Res.* **56:** 2411–2416.

Voeller, H.J., M. Augustus, V. Madike, G.S. Bova, K.C. Carter, and E.P. Gelmann. 1997. Coding region of NKX3.1, a prostate-specific homeobox gene on 8p21, is not mutated in human prostate cancers. *Cancer Res.* **57:** 4455–4459.